

## Radiative transitions in charmonium from $N_f = 2$ twisted mass lattice QCD \*

Y. Chen<sup>a</sup>, D.-C. Du<sup>b</sup>, B.-Z. Guo<sup>b</sup>, N. Li<sup>b</sup>, C. Liu<sup>†c</sup>, H. Liu<sup>b</sup>, Y.-B. Liu<sup>d</sup>, J.-P. Ma<sup>e</sup>,  
X.-F. Meng<sup>f</sup>, Z.-Y. Niu<sup>b</sup>, J.-B. Zhang<sup>g</sup>

<sup>a</sup> Institute of High Energy Physics, Chinese Academy of Sciences, Beijing 100049, China

<sup>b</sup> School of Physics, Peking University, Beijing 100871, China

<sup>c</sup> School of Physics and Center for High Energy Physics, Peking University, Beijing 100871, China

<sup>d</sup> School of Physics, Nankai University, Tianjin 300071, China

<sup>e</sup> Institute of Theoretical Physics, Chinese Academy of Sciences, Beijing 100080, China

<sup>f</sup> National supercomputer center, Tianjin 300457, China

<sup>g</sup> Department of Physics, Zhejiang University, Hangzhou 310027, China

E-mail: chenyl@ihep.ac.cn, liuchuan@pku.edu.cn,  
ddcdragonball@pku.edu.cn, gbz.phy.pku@hotmail.com,  
wyjln7633@126.com, liuhang303@gmail.com, liuyb@nankai.edu.cn,  
majp@itp.ac.cn, mengxf@nsc-tj.gov.cn, niuzy@pku.edu.cn,  
jzbzhang08@zju.edu.cn

We present an exploratory study for charmonium radiative transitions:  $J/\psi \rightarrow \eta_c \gamma$ ,  $\chi_{c0} \rightarrow J/\Psi \gamma$  and  $h_c \rightarrow \eta_c \gamma$  using  $N_f = 2$  twisted mass lattice QCD gauge configurations. The single-quark vector form factors for  $\eta_c$  and  $\chi_{c0}$  are also determined. The simulation is performed at a lattice spacing of  $a = 0.067(2)$  fm and the lattice size is  $32^3 \times 64$  with a pion mass of about 485 MeV. After extrapolation of lattice data at nonzero  $Q^2$  to 0, we compare our results with previous quenched lattice results and the available experimental values.

*The XXIX International Symposium on Lattice Field Theory - Lattice 2011*

*July 10-16, 2011*

*Squaw Valley, Lake Tahoe, California*

\*The numerical computations for this project was performed on the Magic Cube at Shanghai Supercomputer Center and on Tianhe-1A at National Supercomputing Center in Tianjin. This work is supported in part by the National Science Foundation of China (NSFC) under project No.10835002, No.11021092, No.10675101, No.11075167 and No.10975076.

<sup>†</sup>Speaker.

## 1. Introduction

Radiative transitions among various charmonium states are particularly important in the study of charmonium physics. It is also believed to be the ideal hunting ground for exotic hadronic states like the glueballs. Recently, the experimental interests have been revived with the upgrade for the BESIII experiment at BEPCII storage ring [1, 2] which collects charmonium samples that are orders of magnitude larger than ever.

On the theoretical side, charmonium transitions have been studied using various methods. The physical process involves both electromagnetic and strong interactions, the former being perturbative while the latter being non-perturbative. Therefore, non-perturbative lattice calculations are preferred. Radiative transitions of charmonia have been studied comprehensively in quenched lattice QCD for the normal ground state charmonia and for some excited and exotic ones [3]. However, an unquenched lattice study is still lacking. In this paper, we briefly report our unquenched study using  $N_f = 2$  dynamical twisted-mass fermion configurations generated by the European Twisted Mass Collaboration (ETMC). More details of the calculation can be found in Ref. [4].

## 2. Lattice setup and correlation functions

The lattice setup in this calculation is analogous to the vector form factor calculation of pions which has been studied extensively, see e.g. Ref. [8]. This leads to the computation of the hadronic matrix element of the electromagnetic current between the initial and the final charmonium state  $\langle f | j_\mu^{(e.m.)}(x) | i \rangle$ . Although the electromagnetic interaction is perturbative, the matrix element of the current between two hadronic states is in general non-perturbative which requires non-perturbative methods like lattice QCD.

Within the framework of lattice QCD, charmonium states are realized by applying appropriate interpolating operators ( $\mathcal{O}_1$  and  $\mathcal{O}_2$  in the formula below) to the QCD vacuum  $|\Omega\rangle$ . Thus, the computation of the hadronic matrix element naturally leads to the following three-point function:

$$G_\mu(t_2, t; \mathbf{p}_2, \mathbf{p}_1) = \sum_{\mathbf{x}_2, \mathbf{x}} e^{-i\mathbf{p}_2 \cdot \mathbf{x}_2} e^{i\mathbf{q} \cdot \mathbf{x}} \langle \Omega | T \mathcal{O}_2(t_2, \mathbf{x}_2) j_\mu^{(e.m.)}(t, \mathbf{x}) \mathcal{O}_1^\dagger(0, \mathbf{0}) | \Omega \rangle. \quad (2.1)$$

In this formula, interpolating operators which will create/annihilate the appropriate charmonium states are inserted at time slices  $t = 0$  (the source operator) and  $t = t_2$  (the sink operator), respectively. Physically speaking, the three-point function defined above represents a process in which an initial charmonium state with three-momentum  $\mathbf{p}_1 = \mathbf{p}_2 - \mathbf{q}$  created by  $\mathcal{O}_1^\dagger$  makes an electromagnetic transition to the final charmonium state with three-momentum  $\mathbf{p}_2$  annihilated by  $\mathcal{O}_2$  while the three-momentum difference  $\mathbf{q}$  is carried away by the photon.

Inserting a complete set of states between the electromagnetic current operator and the charmonium operators, one finds that, when  $t_2 \gg t \gg 1$ , the desired hadronic matrix element can be obtained once the energies  $E_1, E_2$  and the corresponding overlap matrix elements  $\langle \Omega | \mathcal{O}_2 | f(\mathbf{p}_2) \rangle$ ,  $\langle i(\mathbf{p}_1) | \mathcal{O}_1^\dagger | \Omega \rangle$  are known, all of which can be obtained from corresponding two-point functions for the initial and final charmonium states. For this purpose, two-point correlation functions for the interpolating operators  $\mathcal{O}_i$  for  $i = 1, 2$  are also computed in the simulation:

$$C_i(t, \mathbf{p}) \equiv \sum_{\mathbf{x}} e^{-i\mathbf{p} \cdot \mathbf{x}} \langle \Omega | \mathcal{O}_i(t, \mathbf{x}) \mathcal{O}_i^\dagger(0, \mathbf{0}) | \Omega \rangle \xrightarrow{t \gg 1} \frac{|Z_i(\mathbf{p})|^2}{E_i(\mathbf{p})} e^{-E_i(\mathbf{p}) \cdot \frac{T}{2}} \cosh \left[ E_i(\mathbf{p}) \cdot \left( \frac{T}{2} - t \right) \right], \quad (2.2)$$

where  $Z_i(\mathbf{p})$  is the corresponding overlap matrix element.

With the relevant two-point and three-point functions, the desired hadronic matrix element could be extracted from an appropriate ratio from the two-point and three-point functions:

$$R_\mu(t) = \frac{G_\mu(t_2, t; \mathbf{p}_2, \mathbf{p}_1)}{C_2(t_2, \mathbf{p}_2)} \sqrt{\frac{C_1(t_2 - t, \mathbf{p}_1) C_2(t, \mathbf{p}_2) C_2(t_2, \mathbf{p}_2)}{C_2(t_2 - t, \mathbf{p}_2) C_1(t, \mathbf{p}_1) C_1(t_2, \mathbf{p}_1)}} \simeq \frac{\langle f(\mathbf{p}_2) | j_\mu^{(e.m.)}(0) | i(\mathbf{p}_1) \rangle}{4\sqrt{E_2(\mathbf{p}_2) E_1(\mathbf{p}_1)}} \quad (2.3)$$

where the second equation becomes valid when  $t_2 \gg t \gg 1$ , assuming only the corresponding ground states dominate. In this case,  $R_\mu(t)$  becomes independent of  $t$  and fitting the ratio to a plateau behavior yields the desired hadronic matrix element  $\langle f(\mathbf{p}_2) | j_\mu^{(e.m.)}(0) | i(\mathbf{p}_1) \rangle$ .

In this study, the conserved vector current operator on the lattice is utilized so that no further renormalization is required. Disconnected contributions are neglected as is the case for previous quenched studies [3]. Thus, we only need the charm quark contribution for the electromagnetic current which is proportional to the conserved vector current  $j_\mu(x)$  on the lattice via:  $j_\mu^{(e.m.)}(x) = Q_c j_\mu(x)$  with  $Q_c$  being the electric charge of the charm quark.

### 3. Simulation details

#### 3.1 The simulation setup for $N_f = 2$ twisted mass fermions

Twisted mass fermions at the maximal twist are utilized in our study with two degenerate light flavors in the sea. The framework of maximally twisted mass fermions has been utilized in various studies of lattice QCD and are shown to be highly promising. It offers several advantages when tuned to maximal twist, in particular, the automatic  $\mathcal{O}(a)$  improvement [10] is obtained when the bare untwisted quark mass is tuned to its critical value.

In this study, gauge field configurations using  $N_f = 2$  ( $u$  and  $d$  quark) twisted mass fermion are utilized. Other quark flavors, namely the strange and charm quarks, are introduced as valence quarks as discussed in refs. [5]. In this work, all computations are done using 201  $N_f = 2$  twisted mass fermion configurations at the lattice spacing of  $a = 0.067(2)\text{fm}$  ( $\beta = 4.05$ ) [7]. The size of the lattice is  $32^3 \times 64$  so that the spatial extent of the lattice is about  $2.14\text{fm}$ , a safe value for charmonium physics. In the temporal direction, anti-periodic boundary condition is applied for the quark field while periodic boundary condition is utilized in all spatial directions.

As for the charmonium states, we adopted the Osterwalder-Seiler variant of the twisted mass fermion [11, 6]. Two-point functions are computed as usual for charmonium states  $\eta_c$ ,  $J/\psi$ ,  $\chi_{c0}$ ,  $\chi_{c1}$  and  $h_c$ . Fitting these two-point functions yields the energy for the corresponding charmonium states, both with and without three-momentum. As for the three-point functions, sequential source method is utilized [9]. The results for the two-point and three-point functions are then employed to construct the relevant ratio defined in Eq. (2.3). All errors in this study are estimated using the conventional jack-knife method.

#### 3.2 Charmonium spectrum and dispersion relations

Before computing the transition matrix element, the mass and the energy dispersion relations for the relevant charmonium states are verified. Thanks to the  $\mathcal{O}(a)$  improvement, one would hope to bring the lattice discretization errors under control. In our simulation, it is found that most of

the lattice artifacts are remedied by using the lattice dispersion relations for the charmonium states. We use the mass of  $J/\Psi$  from our simulation to set the bare charm quark mass parameter  $\mu_c$ . Reasonable agreement with the experimental values are found for the mass values.

To get a feeling about the size of the lattice artifacts for the charmonium states with non-vanishing three-momenta, we study the dispersion relations for  $\eta_c$ ,  $J/\Psi$  and  $\chi_{c0}$  states. Our data suggest that the naive continuum dispersion relation is violated, however, if we utilize the standard lattice dispersion relation  $4\sinh^2(E(\mathbf{p})/2) = 4\sinh^2(m/2) + 4Z\sum_i \sin^2(p_i/2)$ , we could describe our data extremely well with the fitted values of  $Z$  for  $\eta_c$  and  $J/\Psi$  rather close to unity.

### 3.3 Form factors for $\eta_c$ and $\chi_{c0}$

In the continuum, the hadronic matrix element  $\langle \eta_c(\mathbf{p}_2) | j_\mu(0) | \eta_c(\mathbf{p}_1) \rangle$  may be parameterized by only one form factor  $f(Q^2)$  as: [3]

$$\langle \eta_c(\mathbf{p}_2) | j_\mu(0) | \eta_c(\mathbf{p}_1) \rangle \equiv f(Q^2)(p_1 + p_2)_\mu, \quad (3.1)$$

where  $Q^2 \equiv -(p_2 - p_1)^2$  is the square of four momentum transfer. To obtain the desired hadronic

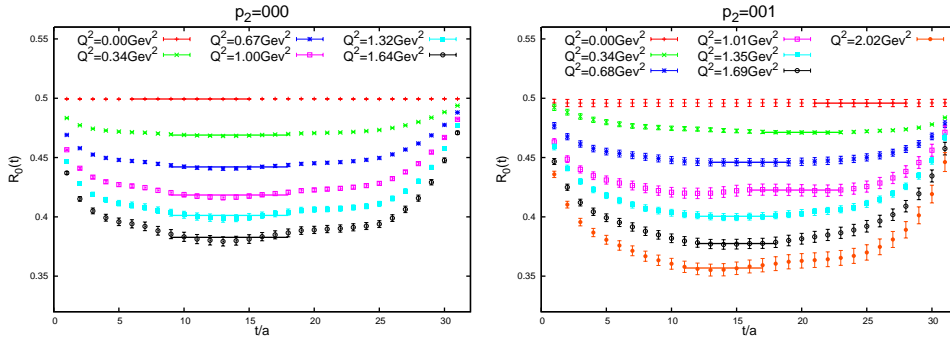


**Figure 1:** The ratio  $R_0(t)$  for  $\eta_c$  with  $\mathbf{p}_2 = (0, 0, 0)$  and  $\mathbf{p}_2 = (0, 0, 1)$ .

matrix element  $\langle \eta_c(\mathbf{p}_2) | j_\mu(0) | \eta_c(\mathbf{p}_1) \rangle$ , we form the ratio defined in Eq. (2.3). In Fig. 1 we display the typical behaviors for  $R_0(t)$  for  $\mathbf{p}_2 = (0, 0, 0)$  and  $\mathbf{p}_2 = (0, 0, 1)$ , respectively. It is seen that clear plateau behaviors have been established from which the form factor  $f(Q^2)$  can be extracted.

The fitted values of  $f(Q^2)$  obtained from the ratio are shown in Fig. 2 versus different values of  $Q^2$  where two different type of symbols stands for  $\mathbf{p}_2 = (0, 0, 0)$  and  $\mathbf{p}_2 = (0, 0, 1)$ , respectively. Following Ref. [3], we fit the data for the form factor with the following function:

$$f(Q^2) = \exp \left[ -\frac{Q^2}{16\beta^2} (1 + \alpha Q^2) \right] \quad (3.2)$$

The fitted parameters turn out to be:  $\alpha = -0.096(6) \text{ GeV}^{-2}$  and  $\beta = 567(2) \text{ MeV}$ . This value of  $\beta$  is larger than the corresponding value  $480(3) \text{ MeV}$  obtained in the quenched approximation in Ref. [3], making the corresponding form factor obtained from our unquenched calculation “harder” (i.e. decays slower with increasing  $Q^2$ ), which can be understood from the effect of unquenching [4]. One can define a squared mean charge radius  $\sqrt{\langle r^2 \rangle}$  with  $\langle r^2 \rangle$  given by

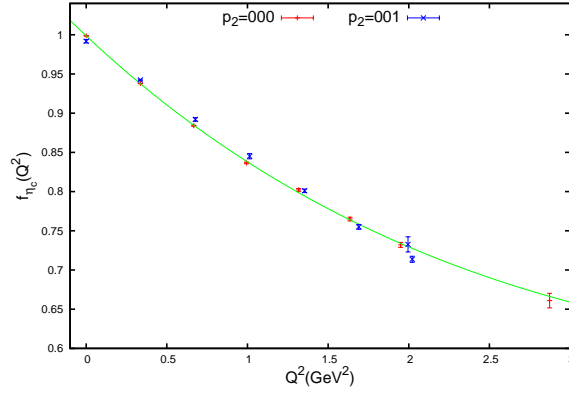


**Figure 2:** The form factor  $f(Q^2)$  for  $\eta_c$ .

$\langle r^2 \rangle = -6f'(0) = 6/(16\beta^2)$ . Our unquenched lattice result then yields  $\sqrt{\langle r^2 \rangle} = 0.213(1)$  fm which is smaller than the corresponding quenched value of  $0.255(2)$  fm in Ref. [3].

The hadronic matrix element  $\langle \chi_{c0}(\mathbf{p}_2) | j_\mu(0) | \chi_{c0}(\mathbf{p}_1) \rangle$  for  $\chi_{c0}$  has the same form of decomposition as that for  $\eta_c$ . In exactly the same manner, we can obtain the form factor  $f(Q^2)$  for  $\chi_{c0}$  except that we have only computed the case  $\mathbf{p}_2 = (0, 0, 0)$ . The data is fitted with the function:  $f(Q^2) = f(0) \exp[-Q^2/(16\beta^2)]$  and the fit parameters are:  $f(0) = 1.0002(5)$  and  $\beta = 510(16)$  MeV. This value of  $\beta$  is also larger than the quenched value of  $393(12)$  MeV from Ref. [3].

### 3.4 Charmonium radiative transitions

#### Transition $J/\Psi \rightarrow \eta_c \gamma$

The matrix element  $\langle \eta_c(\mathbf{p}_2) | j^\mu(0) | [J/\Psi]_r(\mathbf{p}_1) \rangle$  is responsible for the calculation of  $J/\Psi \rightarrow \eta_c \gamma$  transition rate. Here we use the index  $r$  to designate the polarization of the initial  $J/\Psi$  state whose polarization vector is denoted by  $\varepsilon_\gamma(\mathbf{p}_1, r)$ . In the continuum, this matrix element can be decomposed as [3]

$$\langle \eta_c(\mathbf{p}_2) | j^\mu(0) | [J/\Psi]_r(\mathbf{p}_1) \rangle \equiv \frac{2V(Q^2)}{m_{\eta_c} + m_\Psi} \varepsilon^{\mu\alpha\beta\gamma} p_{2\alpha} p_{1\beta} \varepsilon_\gamma(\mathbf{p}_1, r), \quad (3.3)$$

Thus the matrix element is characterized by one form factor  $V(Q^2)$ . By forming the appropriate ratio, relevant lattice results  $\hat{V}(Q^2)$  are extracted from the plateaus of the ratios. The relation of  $\hat{V}(Q^2)$  with its continuum counterpart  $V(Q^2)$  is  $V(Q^2) = 2 \times \frac{2}{3} e \times \hat{V}(Q^2)$ , where the factor 2 comes from the quark and the anti-quark while the factor  $(2e/3)$  is due to the charge of the charm quark. The results for the transition form factor  $\hat{V}(Q^2)$  thus obtained are illustrated in Fig. 3. Following Ref. [3], the data is fitted with the function:

$$\hat{V}(Q^2) = \hat{V}(0) \exp \left[ -\frac{Q^2}{16\beta^2} \right]. \quad (3.4)$$

The resulting fitted parameters we find are as follows:  $\hat{V}(0) = -2.01(2)$  and  $\beta = 580(19)$  MeV. With the values of the transition form factor on the lattice, the  $J/\Psi \rightarrow \eta_c \gamma$  decay width can be obtained:  $\Gamma_{m_{\text{phy}}} = 2.84(6)$  KeV and  $\Gamma_{m_{\text{lat}}} = 1.99(6)$  KeV, where  $\Gamma_{m_{\text{phy}}}$  denotes the result with physical

mass values are utilized, while  $\Gamma_{m_{\text{lat}}}$  stands for using the mass values computed from the lattice directly. This difference arises since our lattice results for the masses for  $J/\Psi$  and  $\eta_c$  do not coincide with their experimental values. Our lattice result for this quantity are to be compared with the value  $\Gamma_{PDG} = 1.58(38)$  KeV quoted by the PDG. Note that the PDG value is an average of CLEO result and the Crystal Ball result, the former being  $1.92(30)$  KeV which is closer to our lattice result while the latter from Crystal Ball being  $1.18(33)$  KeV, smaller than lattice results.

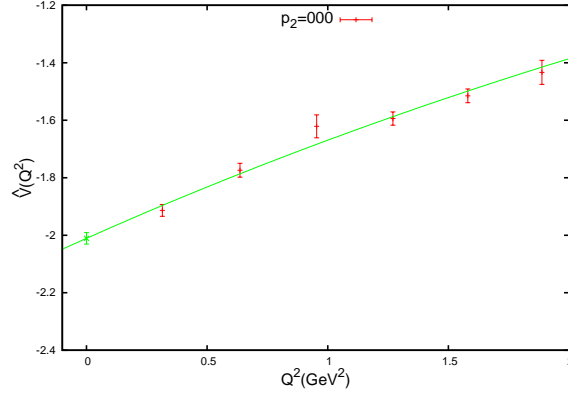


**Figure 3:** The transition form factor  $\hat{V}(Q^2)$  for  $J/\Psi \rightarrow \eta_c \gamma$ .

#### Transition $\chi_{c0} \rightarrow J/\Psi \gamma$

In the continuum, the transition  $\chi_{c0} \rightarrow J/\Psi \gamma$  has a more complicated decomposition [3] which is characterized by two form factors  $E_1(Q^2)$  and  $C_1(Q^2)$ . At the physical photon point with  $Q^2 = 0$ , only the former contributes. Following a similar process, the form factor  $E_1(Q^2)$  can be obtained. We then use the form  $\hat{E}_1(Q^2) = \hat{E}_1(0)(1 + Q^2/\rho^2) \exp[-Q^2/(16\beta^2)]$  to fit the lattice data [3]. At the physical photon point  $Q^2 = 0$ , the decay width for this radiative transition is then obtained:  $\Gamma_{m_{\text{phy}}} = 85(7)$  KeV and  $\Gamma_{m_{\text{lat}}} = 65(4)$  KeV, which is to be compared with the quenched lattice result of  $\Gamma_{m_{\text{phy}}} = 232(41)$  KeV and  $\Gamma_{m_{\text{lat}}} = 288(60)$  KeV.

#### Transition $h_c \rightarrow \eta_c \gamma$

The form factor of  $h_c \rightarrow \eta_c \gamma$  decomposes in the same manner as that of  $\chi_{c0}$ , however, the signal is much noisier. We fit the data for the corresponding form factor  $\hat{E}_1(Q^2)$  with a functional form  $\hat{E}_1(Q^2) = \hat{E}_1(0) \exp[-Q^2/(16\beta^2)]$ . [3] The physical decay width for the transition is given by:  $\Gamma_{m_{\text{phy}}} = 234(12)$  KeV and  $\Gamma_{m_{\text{lat}}} = 210(13)$  KeV. The corresponding quenched lattice values are:  $\Gamma_{m_{\text{phy}}} = 601(55)$  KeV and  $\Gamma_{m_{\text{lat}}} = 663(132)$  KeV, both of which are about a factor of 3 larger than our unquenched result, though the errors are somewhat large. The lattice results for this decay can now be compared with the recent measurement at BES-III: [12]  $\Gamma(h_c \rightarrow \eta_c \gamma) = 396(294)$  keV. The agreement within a large error is seen although improvements from both experiment and lattice calculations are required to cut down the large uncertainties for this quantity.

## 4. Summary and conclusions

In this exploratory study, we calculate the form factors for some of the ground state charmonia and their radiative transitions using unquenched  $N_f = 2$  twisted mass fermions. Our study focuses

**Table 1:** Summary of the results obtained in this work. Also listed are the corresponding results from quenched lattice QCD [3]. Experimental values or values from PDG are also listed whenever available.

	$\Gamma_{m_{\text{phy}}}/\Gamma_{m_{\text{lat}}} [\text{keV}]$			$\beta [\text{MeV}]$	
	$J/\Psi \rightarrow \eta_c \gamma$	$\chi_{c0} \rightarrow J/\Psi \gamma$	$h_c \rightarrow \eta_c \gamma$	$\eta_c$	$\chi_{c0}$
PDG	1.58(38)	119(11)	396(294)	-	-
This work	2.84(6)/1.99(6)	85(7)/65(4)	234(12)/210(13)	567(2)	510(16)
Ref. [3]	2.57(11)/1.61(7)	232(41)/288(60)	601(55)/663(132)	480(3)	393(12)

on the form factors for  $\eta_c$ ,  $\chi_{c0}$  and the  $J/\Psi \rightarrow \eta_c \gamma$ ,  $\chi_{c0} \rightarrow J/\Psi \gamma$ ,  $h_c \rightarrow \eta_c \gamma$  radiative transitions. It is verified that, by using lattice dispersion relations instead of the naive continuum ones, the lattice artifacts for these charmonium states are well under control. By computing various appropriate ratios of the three-point functions to the two-point functions, hadronic matrix elements for these transitions are obtained at various values of  $Q^2$ . Using the parameterized form in terms of relevant form factors, we obtain the lattice results for the relevant form factors and the radiative decay widths for these channels. Our results are summarized in Table 1 which are to be compared with those obtained in previous quenched lattice studies and experimental values.

In this preliminary study, we simulate at only one lattice spacing and sea quark mass, and neither chiral nor continuum extrapolation is made. We argued that, thanks to the automatic  $\mathcal{O}(a)$  improvement, the lattice artifacts is under control. With the experience gained in this study, it is feasible to study charmonium radiative transitions in a more systematic manner (more lattice spacings, more pion mass values etc.) using unquenched lattice QCD in the future.

## References

- [1] M. Ablikim et al. (BESIII Collaboration). *Nucl. Instrum. Methods Phys. Res., Sect. A*, 614:345, 2010.
- [2] K.T. Chao and Y. Wang ed. *Int. J. Mod. Phys. A, Suppl. 1*, 24:1, 2009.
- [3] J.J.Dudek, R.G.Edwards, and D.G.Richards. *Phys. Rev. D*, 73:074507, 2006; J.J.Dudek, R.G.Edwards, and C.Thomas. *Phys. Rev. D*, 79:094504, 2009.
- [4] C. Chen et al. *Phys. Rev.*, D84:034503, 2011.
- [5] R. Frezzotti and G.C.Rossi. *JHEP*, 0410:070, 2004; B. Blossier et al. (ETM collaboration). *JHEP*, 0804:020, 2008; B. Blossier et al. (ETM collaboration). *JHEP*, 0907:043, 2009.
- [6] C. Alexandrou et al. (ETM collaboration). *Phys. Rev. D*, 80:114503, 2009.
- [7] B. Blossier et al. *Phys. Rev.*, D82:114513, 2010.
- [8] R. Frezzotti, V. Lubicz, and S. Simula. *Phys. Rev. D*, 79:074506, 2009.
- [9] F.D.R. Bonnet, R.G. Edwards, G.T. Fleming, R. Lewis, and D.G. Richards. *Phys. Rev. D*, 72:054506, 2005.
- [10] R. Frezzotti and G. C. Rossi. *JHEP*, 08:007, 2004.
- [11] K. Osterwalder and E. Seiler. *Ann. Phys.*, 110:440, 1978.
- [12] The BESIII Collaboration. *Phys.Rev.Lett.*, 104:132002, 2010.